Computational Fluid Dynamics Analysis of Self-Sustained Laminar Flow Oscillations in Singular Grooved Ducts

Yifei Chen, Stephen Tullis

Department of Mechanical Engineering, McMaster University, Hamilton, Canada

cyifei@umich.edu

Abstract. Research Background: Modeling oscillatory flow in singular grooved ducts within the laminar regime provides insight into fluid mechanics that could enhance applications such as heat transfer in nuclear reactors. Previous research has identified pulsations in grooved channels under turbulent conditions with high Reynolds numbers, contributing to enhanced heat exchange efficiency. These pulsations are influenced by the axial flow in and out of the main channel from a continuous groove. Contribution of This Study: This study extends the understanding of flow oscillations to simpler geometries and lower Reynolds numbers, specifically within a laminar flow regime capped at a Reynolds number of 2,000. By simplifying the duct geometry to a rectangular main channel with a singular continuous groove, the research employs computational fluid dynamics tools, primarily OpenFOAM, facilitated by Compute Canada's clusters. It investigates the fluid flow characteristics—strength, frequency, velocity gradient, and oscillation behaviours—associated with the geometry of the gaps and channels. This approach helps in pinpointing the dependency of flow characteristics on specific geometric configurations, potentially laying groundwork for optimizing designs in practical applications.

Keywords: Computational fluid dynamics, Low-Reynolds number, Laminar flow, Flow pulsations, OpenFOAM, Clusters.

1. Introduction

In the nuclear industry, a deep understanding of the flow characteristics within reactor cores is crucial for enhancing the safety and efficiency of nuclear reactors. The CANDU-6 nuclear reactor, a Canadian reactor with a unique horizontal core configuration [1], exhibits particularly complex internal flow phenomena. Previous research has indicated the presence of flow pulsations within rod bundles with axial flow (as depicted in Fig. 1). As the coolant (heavy water) enters the fuel bundles, some of the fluid enters the gaps between the bundle walls, causing internal oscillations [2-5]. These oscillations are predominantly crossflow rather than radial. Similar oscillatory flows have also been observed in simpler geometries, such as a single channel with a continuous groove [3-10]. Thus, by simplifying the geometry to a single rectangular main channel with a groove, this study aims to simulate these flow pulsations and explore how their characteristics (mainly strength and frequency) are influenced by the geometry of the gaps and the channel as well as the bulk velocity of the inflow. Although such flow patterns have been observed in laminar flows experimentally, detailed quantitative information could not be measured without disturbing the flow. Our group has also observed similar flows using computational fluid dynamics models, which broadly align with the limited experimental results [11, 12]. This research is important to the nuclear industry, as it helps engineers optimize reactor designs and enhance operational safety.

Main Research Questions Addressed: The main issues addressed in this paper involve ensuring the accuracy of simulation results in a high-density grid environment. To achieve this goal, it is necessary to construct a high-density grid system comprising millions of block meshes. Such a high-precision grid configuration will significantly increase the CPU and memory load on local computers, leading to exponential growth in computational time. Therefore, simulations for testing and development phases will be conducted on local computers, while large-scale production runs will be executed on substantial clusters through ComputeCanada. This arrangement aims to optimize resource usage, ensure the efficiency and precision of the simulation process, and address the challenges posed by local resource limitations.

This paper outlines a robust methodology utilizing the OpenFOAM open-source CFD toolbox to simulate flow dynamics, which are then visualized using the third-party platform ParaView. To ensure the precision required for these simulations, we have meticulously designed a high-density grid system incorporating millions of block meshes, accommodating the complex dynamics of flow within engineered channels. Recognizing the intensive computational demands of these high-accuracy simulations, we leverage the extensive computational power of large clusters provided by ComputeCanada. This strategic use of resources effectively overcomes the limitations posed by local computational infrastructures. Additionally, this research goes beyond mere simulation, as it thoroughly investigates the impact of channel and gap geometries on the characteristics—specifically the intensity and frequency—of flow pulsations, thereby providing deeper insights into fluid dynamics within specialized configurations. Through this approach, we deliver a comprehensive analysis of flow behavior, contributing valuable data and interpretations to the field of fluid dynamics.

Contributions of This Paper:

1) We utilize the open-source CFD toolbox OpenFOAM to simulate oscillatory flow dynamics and display the results through the third-party platform ParaView.

2) To meet the demands for simulation accuracy, we have designed a high-density grid system comprising millions of block meshes.

3) Due to the significant demand for computational resources by high-accuracy simulations, we employ large clusters via ComputeCanada for production runs, effectively addressing the limitations of local computational resources.

4) This research not only simulates flow pulsations but also investigates how the intensity and frequency of these pulsations are influenced by the inflow bulk velocity in a singular grooved duct.

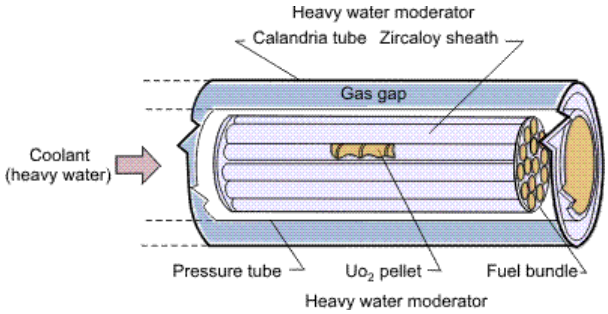

Figure 1. Fuel bundle in a fuel channel [1]

2. Related Work

2.1. Turbulent Experiments

Scientists conducted experiments based on different simplified geometries to better understand the flow instability in the channel. Among those scientists [2-6], Hooper, Rehme, and Meyer did extraordinary work, focusing on analyzing flow pulsations in the turbulent regime, further proving the authenticity of the existence of flow oscillations.

In 1984, Hooper and Rehme [2] performed measurements in a geometry as in Fig. 2, in which the geometry setup has several rods installed inside a rectangular channel parallelly. It was shown that an energetic and almost periodic flow pulsation exists through the gaps between the rods and between rods and channel walls. Based on the results obtained, Hooper and Rehme concluded the frequency of pulsation was proportional to the Reynolds number. As the Reynolds number within the turbulent flow regime increases, the flow pulsation frequency increases. This experimental conclusion is critical for our further research orientation to determine the authenticity of this relationship in the laminar regime.

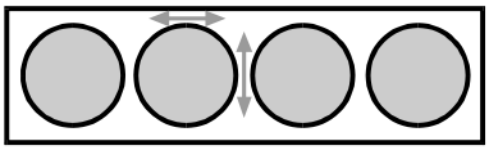

Figure 2. Hooper and Rehme's experiment geometry [2]

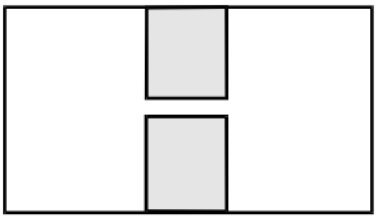

Figure 3. Meyer and Rehme's experiment geometry in 1994 [3]

Meyer and Rehme's experiment geometry in 1994 [3] was a rectangular interconnected channel (refer to Fig. 3). Meyer and Rehme investigated the flow passing through the channel to search for the necessary geometric boundary conditions for the occurrence of periodic flow pulsations. According to their finding with a foundation of results, it was concluded that large-scale quasi-periodic flow pulsations could be detected in all geometries where the gap depth was more than twice its width. This experimental conclusion is also critical for our further research orientation, determining one of the preconditions of the occurrence of oscillatory flow. Furthermore, Meyer and Rehme's 1994 experiment [3] also proved that the frequency of these pulsations increased with both decreasing gap depth and decreasing width. One year after they discovered the effects of the ratio of gap depth and its width to the flow instability, the experiment geometry in 1995 [4] was changed to a singular main channel with a continuous groove for further study, as shown in Fig. 4. It is exactly the geometry we applied in our research [4, 12], which is an even simpler geometry compared to the one Meyer and Rehme did in 1994.

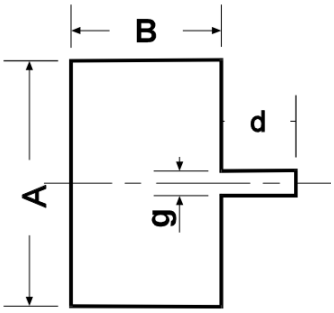

Figure 4. Meyer and Rehme's further-study geometry in 1995 [4]

Refer to Fig. 5, which shows the region of the slot (dark) and part of the main cross-section (light) of a flow channel. Stable vortices keeping a constant spacing independent of the flow velocity move axially through the slot and are driven by the higher velocity outside of the slot.

Figure 5. Visualization of Eddies moving from left to right in the longitudinal slot [4]

2.2. Laminar Experiments

Although people used to think flow instability only appeared in the case of turbulent flow, oscillatory flow was found to occur in the laminar regime as well, under some particular preconditions. Due to the initial thought that no flow oscillations existed in the laminar regime, most scientists were studying the turbulent flow region. They seldom did laminar experiments to observe self-sustained

flow oscillations. Yet, Gosset and Tavoularis [11] and Ethan Sun [12] are the minority who studied the laminar experiment, and Sun worked on this kind of research in 2020.

In 2006, Gosset and Tavoularis's experiments [11] in laminar flow in a rectangular channel containing a cylindrical rod (see Fig. 6) revealed flow instability in the form of weak pulsations across the gap between the rod and the channel wall. Therefore, it has been proved that flow oscillations can occur in the laminar regime. Gosset and Tavoularis injected dye into the interspace, which is beneath the upper wall of the channel and above the cylindrical rod, to observe its stream along the length of the duct in the laminar flow regime. According to their experimental conclusion, the flow instability occurs as the Reynolds number reaches a critical value within 2,000 at the steady state; in the meantime, its oscillation tends to increase at a constant Reynolds number as the gap (the interspace between the cylindrical rod and the upper wall of the channel), δ as referred to in Fig.6, diminishes. In the other case, if only the Reynolds number is varied, the geometry and other conditions remain unchanged, and the pulsations become more vigorous and develop as the Reynolds number is increased.

As shown in Fig. 7, the bulk flow is from the left to the right along the length of the channel. The pulsations develop, first into hairpin-shaped patterns, then into quasi-periodic laminar vortices, and the oscillatory flow is clearly formed eventually as the Reynolds number is increased to a critical value, as mentioned.

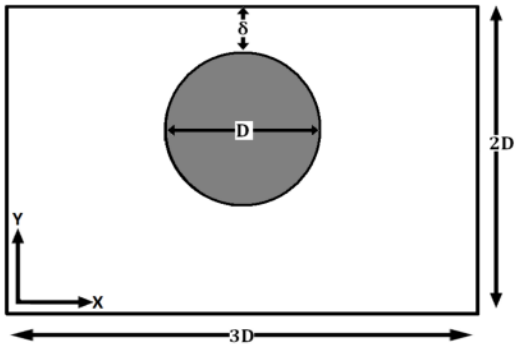

Figure 6. The geometry of a rectangular channel with a cylindrical core used by Gosset and Tavoularis [11]

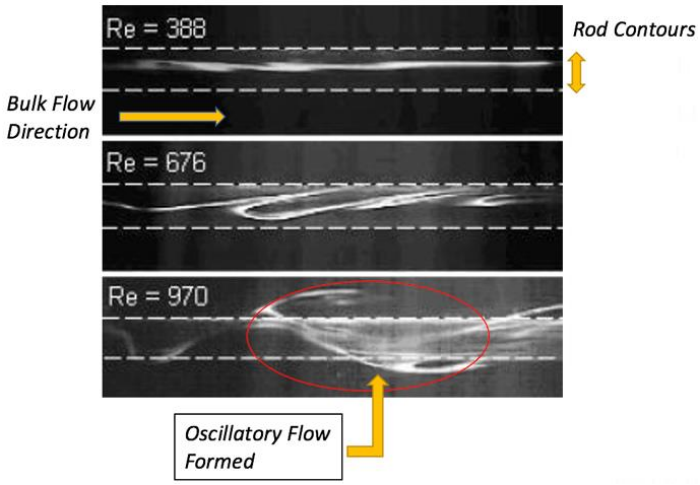

Figure 7. The Formation of Oscillatory Flow with Reynolds Number [11]

Sun's study [12] of simulation offered the base setup for the initial case run. Our research will continue to work for flow oscillations simulation and analysis based on his previous work. For more information about Ethan Sun's research in 2020 and results, please refer to his final individual study report, "Modeling Laminar Oscillatory Flow in Single Grooved Channels."

3. Methodologies

The research simulation would utilize OpenFOAM. As mentioned, this research continues Ethan Sun's study in 2020. The initial base setup refers to his model, so the correctness of the flow simulation in a singular grooved duct can be validated. Meanwhile, some basic validations of the model would be tested before simulating the oscillatory flow. All the following setups are for computing a high degree of fidelity to the actual system.

3.1. Geometry and Dimension of the Experimental Duct

The geometry investigated in this research is a rectangular main channel with a singular continuous slot on the side. This geometry is derived from Meyer and Rehme's work [4], which is the most straightforward geometry to produce flow pulsations. Specifically, it is the exact geometry shape that Meyer and Rehme experimented with in 1995, but with different dimensions of both the main channel and the groove. Furthermore, our group modelled the flow oscillations based on this duct geometry for the laminar case rather than for turbulent experiments like Meyer and Rehme. The dimensions of the entire duct will be modified for the research study requirements, and the slot's dimension should be altered and iterated to obtain self-sustaining oscillations. Here, we focus on the first trial of the experimental geometry as in Fig. 8. The detailed geometry dimensions will be summarized, and their labels listed in Table 1, as referred to in Fig. 8. The total length of the channel is 8 meters along the z-axis (Fig. 9). The depth of the slot, d (30mm), is set more than twice its width, g (12mm), since there is a precondition for flow oscillation formation.

Table 1. Dimensions of the cross-section of the geometry

Geometry	A	B	d	g
Trial 1	66mm	30mm	30mm	12mm

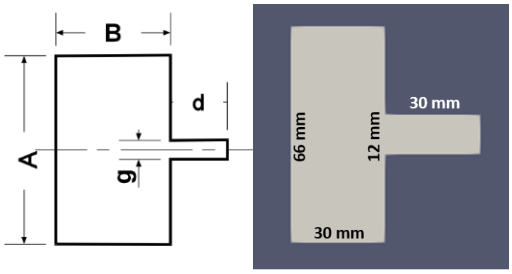

Figure 8. The experimented cross-sectional geometry in the research. The orientation of flow is into the page (Photo credit: Original)

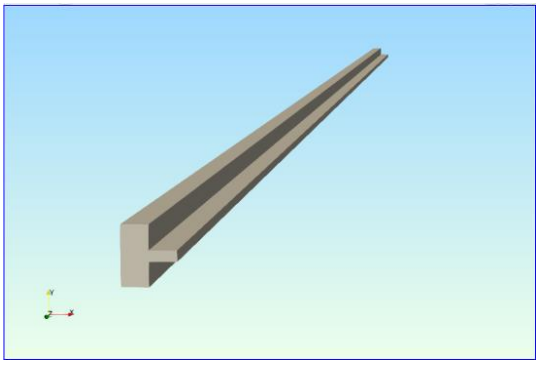

Figure 9. The oblique projection of the experimented geometry (Photo credit: Original)

3.2. Mesh and Grid Independence

The property of the fluid in the simulation is incompressible and isothermal, which is water at 25℃, with a kinematic viscosity of 8.926×10^{-7} squared-meter per second. The shape of grids used for meshing is the rectangular block structure, and the mesh set is compromised in CFD analysis. A mesh with smaller grids set for elbows or critical regions is beneficial to the accuracy of the results. Yet,

the computer requires a powerful CPU and is time-consuming for calculations. Hence, the dimension of each grid in a mesh is one of the criteria for base setup in this project. The dimensions and numbers of the grid set for the cross-section of the channel are summarized in Table 2. Furthermore, cell spacing was applied to refine the cells close to the walls or the edge of the gap for better resolution with high-velocity gradients. The independence of the meshing was tested by either varying cell sizes or varying cell spaces, so the mesh density could be varied to get similar simulation results.

Table 2. Dimensions in millimeters and NUM. of the grid set

Trial 1	**A**	**B**	**d**	**g**	**Length**
# of grids	75	38	50	25	8000
Grid Dimension	0.88	0.79	0.6	0.48	1

3.3. Time Range Control of the Simulation

Controlling the time interval is one of the critical setups for successfully capturing the flow oscillations. Once the time interval is reduced to be minor, more data points are captured in one cycle period, so more potential circumstances of oscillatory flow can be observed, which a long-time-interval setting cannot do. The summary of the time control file is in Tables 3 and 4, and the independence of the timestep was validated by decreasing its size while monitoring the flow oscillation frequency for each case.

The general time control setup (refer to Table 3.) gives an overview of the simulation of the flow inside the channel. Still, the detailed information on flow pulsations has yet to be determined with various channel dimensions, but the characteristics of Trial 1 were simulated and obtained. Based on the consequences captured every 10 seconds, the conclusion that can be made is whether the flow oscillations occur. Nevertheless, the detailed information can be analyzed in flow pulsations, if the time interval of the simulation is reduced to 4 timesteps every second. The time control setup in Table 4. gives a deeper view of the oscillatory flow in and out of the groove in both the streamwise and spanwise directions. Four timestep plots every second can provide a relatively completed progress of how the flow oscillates in one period.

Table 3. General Time Control Setup. All units are in seconds

Trial 1	
Start Time	0
End Time	800
Delta Time	0.002
Write Interval	10 (every 10th time step)
Courant Number	0.008

Table 4. Detailed Time Control Setup among time spans. All units are in seconds

Trial 1	
Start Time	470
End Time	500
Delta Time	0.002
Write Interval	0.25 (4 timesteps, per second)
Courant Number	0.008

3.4. Governing Equations

The conservations of mass and momentum are applied, and the governing equations involved in this research are the Reynolds number equation (Eqn. 1), Continuity equation (Eqn. 2 and 3), Momentum equations (Eqn. 4), which are Navier-Stokes equations for an incompressible, Newtonian fluid. The equation 4 is a laminar flow example, and it can be extended to define a stream function for incompressible 3D fluid. Since this study is proposed to investigate the laminar flow instabilities with no turbulent situations involved in the simulation, the Euler equations can be simplified to the

incompressible continuity equations. Moreover, the energy transfer inside the channel must be neglected since the flow simulation is considered in isothermal situations.

$$Re = \frac{U_b D_h}{\upsilon} \tag{1}$$

$$\nabla \cdot u = 0 \tag{2}$$

$$\frac{\partial \rho}{\partial t} + \frac{\partial (\rho u)}{\partial x} + \frac{\partial (\rho v)}{\partial y} + \frac{\partial (\rho w)}{\partial z} = 0 \tag{3}$$

$$\rho(\frac{Du}{Dt} + (u \cdot \nabla)u) = -\nabla p + \rho g + \mu \nabla^2 u \tag{4}$$

4. Experiment and Analysis

4.1. Experimental Setup

4.1.1 Boundary conditions and bulk velocities

The study case is laminar for this entire project. The bulk velocity at the inlet is set as 0.02m/s (Case a), 0.03m/s (Case b), 0.04m/s (Case c) and 0.05m/s (Case d), flowing along the 8-meter length channel. The inlet pressure gradient sets at zero, and the outlet pressure is uniformly zero. The velocity at the outlet is set as a zero gradient, and the flow velocity near the walls is set at zero due to the no-slip condition. The Reynolds number is controlled within 2000, based on the hydraulic diameter of the geometry, to maintain the flow in the laminar regime. The detailed information on all boundary conditions is listed in Table 5 for reference.

Table 5. Boundary Conditions Setting

TRIAL 1			
Velocity Setting			
Bulk Velocity		0.02m/s (Case a), 0.03m/s (Case b), 0.04m/s (Case c), 0.05m/s (Case d)	
Reynolds Number (respect to hydraulic dia.)		About 750, within 2000	
Inlet Velocity (Case c)	Outlet Velocity Gradient	Velocity at Channel Walls	Velocity at Groove Walls
0.04m/s	Zero	All 0m/s	All 0m/s
Pressure Setting			
Inlet Pressure Gradient	Outlet Pressure	Pressure Gradient at Channel Walls	Pressure Gradient at Groove Walls
Zero	0	All Zero	All Zero

4.1.2 Support organization

The simulation will be run on local computers for testing and development, but the production runs will be done on a cluster maintained by ComputeCanada. These machines have over 30,000 cores, yet our jobs would probably have around 50-100. Using local computers to set up the fluid model's initial run and validation is possible, but finalizing the calculated results would take several hours. In the meantime, the computational time will be extraordinarily time-consuming. For example, running several days or even weeks for one simulation case in hundreds of seconds, as either the dimension of the grid or the time interval is modified to be so small that the accuracy of the simulation will allow us to capture those faint flow pulsations (continuous changes of velocity gradients along the channel). Therefore, big computers are required to boost computational speed and make time efficient.

4.2. Result Analysis

4.2.1 Initial analysis

The results obtained through the simulation (Fig. 10, 11, and 12) confirm that reaching the steady state of the flow requires both time and distance to develop, which is the prerequisite for forming self-sustained laminar flow oscillations.

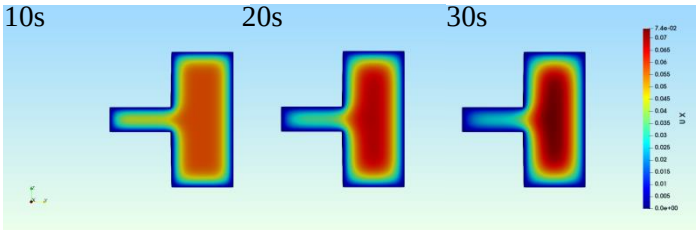

Figure 10. The developing process of flow velocity in x-axis. The cross section of outlet (x=10m) along the x-axis at time 10s, 20s and 30s respectively (Photo credit: Original)

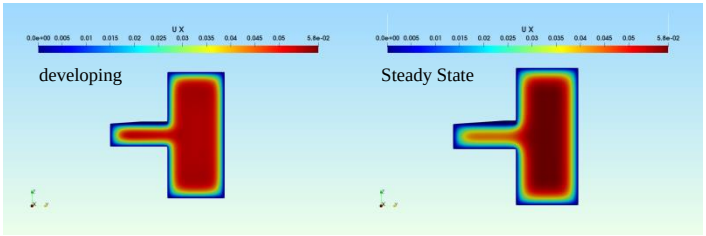

Figure 11. The x-axis flow velocity at x=0.2m (developing) and x=5m (steady state), as t=10s (Photo credit: Original)

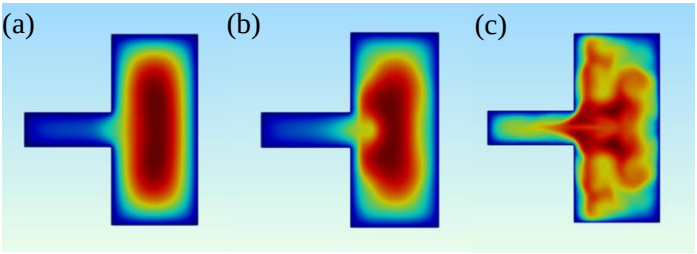

Figure 12. The developing process of flow velocity in x-axis. The cross-section plots of positions (a. x=3.0m, b. x=3.8m, c. x=4.5m) along the x-axis at time t=470s (Photo credit: Original)

Based on the theory of boundary condition, the flow velocity should be zero at walls due to the no-slip condition, which can be proved from the graphs of Fig. 10 and Fig. 11. One exciting phenomenon is the flow velocity in the groove is always slower than the main channel. Its velocity inside the groove would be even smaller as time and distance pass. It happens because the width of the slot is much narrower than the main channel, so the friction from the wall is more significant. The streamwise velocity of the oscillation at the centerline of the main channel is approximately 0.083m/s, shown in the red contour, which is nearly two times the inlet bulk velocity. It proves the truth of the conservation of mass in a domain. Since the total mass flow rate should be constant at the inlet and outlet, the centerline velocity will be faster than the inlet velocity due to the low velocity inside the groove caused by the skin friction at walls. As the flow is developed and at the steady state, at some specific locations, both the streamwise and spanwise velocities near the gap edge of the groove start to oscillate periodically. This is the rudiment of the formation of the messy flow oscillations. Referring to Fig. 12, it can be visualized that the periodic oscillatory flow requires a specific distance to form inside the channel. Similarly, time is a factor that helps us capture the oscillations at a fixed position.

4.2.2 Detection of self-sustained flow oscillations

According to the simulation results, self-sustained laminar flow oscillations could be captured from the trial one geometry, as the inlet bulk velocities are 0.03m/s, 0.04m/s or 0.05m/s. While the

oscillatory flow failed to be observed in 600 seconds, if the bulk velocity is 0.02m/s, it might require more time to develop till the messy flow pulsation can be observed. However, if the scale set is micro enough, some feeble periodic fluctuations at the developing stage still exist and can be detected. Hence, we can speculate that this periodic self-sustained flow oscillation occurs mainly depending on the geometry of the channel but not the bulk velocity at the inlet. It only requires more time to complete the development until visible messy flow oscillations form, if the initial flow velocity is less than 0.03m/s. Future research should focus on applying varying dimensions of this geometry to see whether the self-sustained oscillatory flow will occur again in the flow rate cases listed in Table 5.

Refer to Figure 12., the flow enters the domain and flows from the left to the right until the 8-meter-length outlet. It shows the velocity contours of the cross-sectional channel plate cut along the y-axis centerline, where the inlet bulk velocity enters the domain at 0.04m/s. As referred to in Fig. 13, the top half of the contour is within the main rectangular channel, and the bottom half displays the distribution of different flow rates inside the groove. The self-sustained periodic oscillatory flow is captured in the Trial 1 Case c scenario, and its original point of the start of oscillations remains fixed among the range of 2.40 and 2.45 meters downstream from the inlet, according to Table 6.

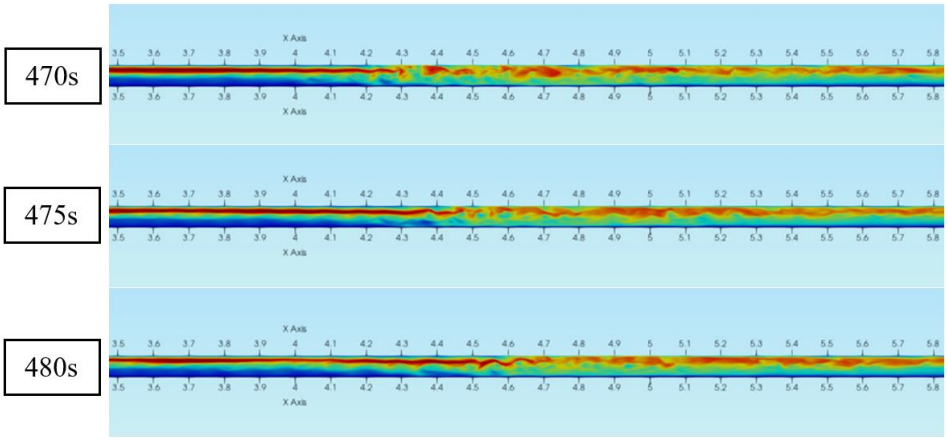

Figure 13. The streamwise velocity contours of self-sustained periodic flow pulsations from Trial 1, Case c. The snapshots are taken at 470s, 475s, and 480s from the top to the bottom, respectively. The view is cut along the y-axis (Photo credit: Original)

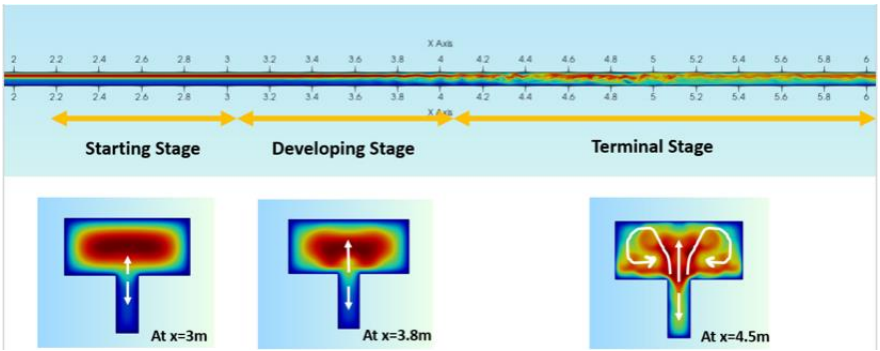

Figure 14. The overview of stages in the oscillation development (Photo credit: Original)

4.2.3 Oscillation development process

As shown in Figure 13, the progress of the oscillation formation can be divided into three stages: “Starting Stage,” “Developing Stage,” and “Terminal Stage.” As the flow is at a steady state in the scenario of Trial 1. Case c., the spanwise velocity of the oscillatory flow oscillating between the main channel and the groove is less than 0.1% of the bulk velocity until about the range of 2.70 and 2.90 meters downstream in different time points, where the domain before that range is called the “Starting Stage” of the oscillation formation. Those small amplitude flow fluctuations occur close to the groove edge at the starting stage. The “Developing Stage” is a range of domains where the spanwise velocity increases to about 1% of the bulk velocity, and its original axial flow transits into the quasi-periodic

oscillatory flow, with intermediate oscillation amplitudes at the groove edge but is less affected by the main channel flow. The range of the domain at this stage is from about 3.00m to 4.00m. After approximately 4.00 meters, in this case, it is the "Terminal Stage." The amplitude of the spanwise oscillation velocity will significantly increase to nearly 10% of the bulk velocity. The main channel flow will be wrapped, and its flow profile will be disrupted.

Table 6. The locations of oscillation development stages in varying times

Trial #1 Case #c	Starting Stage Location (m)	Developing Stage Location (m)	Terminal Stage Location (m)
@ t=470s	2.392-2.712	2.712-4.120	4.120
@ t=471s	2.408-2.744	2.744-3.920	3.920
@ t=472s	2.464-2.776	2.776-3.904	3.904
@ t=473s	2.416-2.816	2.816-3.896	3.896
@ t=474s	2.440-2.848	2.848-4.032	4.032
@ t=475s	2.408-2.888	2.888-3.480	3.480
@ t=476s	2.432-3.000	3.000-4.096	4.096
@ t=477s	2.464-2.672	2.672-3.528	3.528
@ t=478s	2.432-2.712	2.712-3.624	3.624
@ t=479s	2.448-2.744	2.744-3.776	3.776
@ t=480s	2.496-2.744	2.744-4.160	4.160

Table 7. The locations of oscillation development stages at t=470s with different study cases (a. x=3.0m, b. x=3.8m, c. x=4.5m)

Trial #1 @470s	Starting Stage Location (m)	Developing Stage Location (m)	Terminal Stage Location (m)
A (0.02m/s)	3.672-5.664	5.664-7.496	7.496
B (0.03m/s)	2.440-3.232	3.232-4.240	4.240
C (0.04m/s)	2.200-2.784	2.784-3.960	3.960
D (0.05m/s)	2.016-2.784	2.784-3.832	3.832

In general, the progress of flow oscillation development in the scenario of the same geometry and bulk velocity will have similar ranges of the domain of stages as time goes by if the flow is at the steady state. As referred to in Table 6., in the ten-second data collection, the locations of the "Starting Stage" (2.436m to 2.787m), "Developing Stage" (2.787m to 3.867m), and "Terminal Stage" (3.867m) are altered less than about 0.5 meters. Thereby, the stages of oscillation formation can be speculated at different times for the same scenario, which is less dependent on the time period.

All the result data listed in Table 7 were obtained from the simulation. It shows that lower bulk velocity requires a longer distance and time to develop fully; otherwise, no oscillations will be captured (refer to Table 7., Case a.). For example, the oscillation is challenging to capture as Ubulk is 0.02m/s, since the oscillations go to form at the end of the channel. However, the flow oscillation has been messy at nearly half of the total length of the channel when the inlet bulk velocity is 0.03m/s, 0.04m/s or 0.05m/s. Therefore, we can conclude that a higher bulk velocity can accelerate the

formation of flow oscillations. As the bulk velocity is 0.02m/s, it is more likely that the flow inside the channel is not fully developed or at a steady state, so oscillatory flow delays occur. In that case, a longer distance or flow time is critical for capturing the flow pulsations. If the flow is fully developed, as in the cases of b, c, and d, the displacement of each stage's domain should be similar, but the flow rate should differ. Therefore, it also can be concluded that the positions of the "Starting Stage," "Developing Stage," and "Terminal Stage" ranges might be inversely proportional to the flow rate at the steady state, according to Table 7.

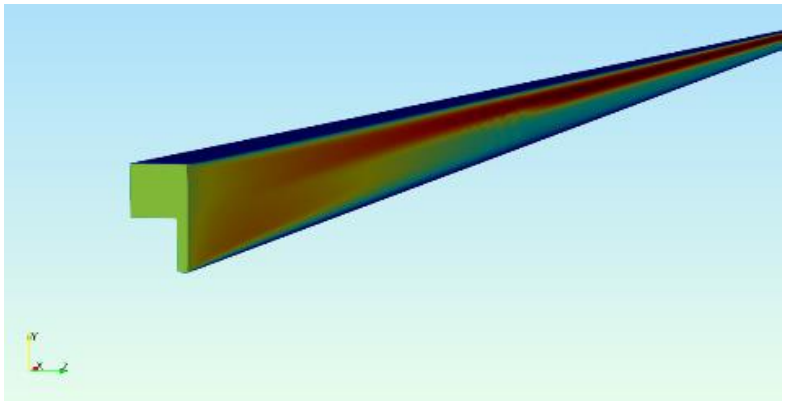

Figure 15. The cross-section view cut along the y-axis (Photo credit: Original)

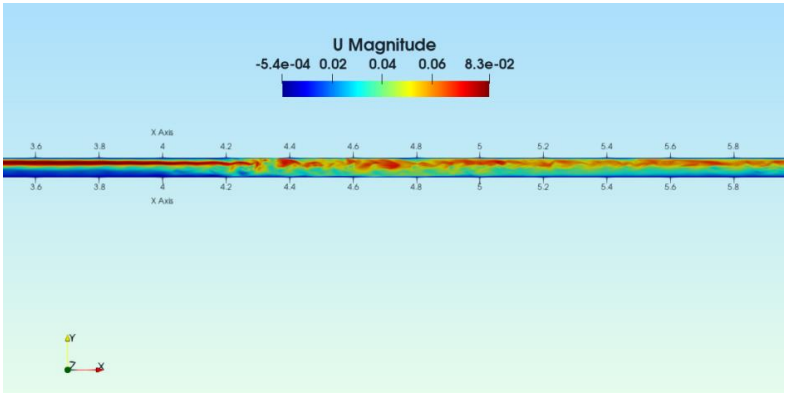

Figure 16. Flow velocity at t=470s along the x-axis with respect to the cross-section view cut along the y-axis. Trial 1. Case c (Photo credit: Original)

As shown in Fig. 15, the analysis of the cross-section view is cut along the y-axis at the centerline. Fig.16 displays the velocity contours along the duct, when the flow enters the inlet at 0.04 m/s. The initial inlet velocity is uniform at either the main channel or groove. Yet, it tends to develop as displacement increases with respect to the domain due to the boundary condition, making the fluid flow quicker in the main channel than in the groove. According to Ethan Sun's post-simulation, the self-sustained oscillatory flow in the laminar regime can be visually captured around 500 seconds with a sufficient-long distance for the flow to complete the development [12]. However, the local computer run cannot simulate such an extended period, which occupies CPU, storage and time [13]. The clear visible flow oscillations were obtained by submitting the jobs and running them on ComputeCanada clusters. Our group captured the flow oscillation starting at about x=2.4m and becoming chaotic at x=4.12m, as referred to in Fig. 16 and 17. Sometimes, those pulsations have a relatively high frequency to make them undetectable. To detect detailed information on the pattern of flow oscillations in one period, a cluster of computers should calculate and simulate more plots in one-quarter of a second. The initial flow is so fast in the groove that it is forced out of the groove into the main channel near the start of the channel, but it settles down to a laminar profile further downstream before the flow oscillations occur at where is nearly a half of the total length of the channel.

Around the displacement at x=4.12m, the spanwise velocity normal to the x-axis (refer to Fig. 17) is also abnormal due to the flow pulsation along the channel. Fig.17 shows the variation of the spanwise velocity along the duct, being like a pattern of sine wave, with one segment having a positive y-velocity and the next being negative in a circulation from the domain of x=2.392m downstream to the outlet. Capturing visible laminar flow pulsations in the channel and analyzing its formation requisites are the ultimate goals of our research, and it should be worked on and done in this research study. In the future, various dimensions of the main channel or groove should be researched to make a general conclusion in oscillatory flow in a singular grooved duct.

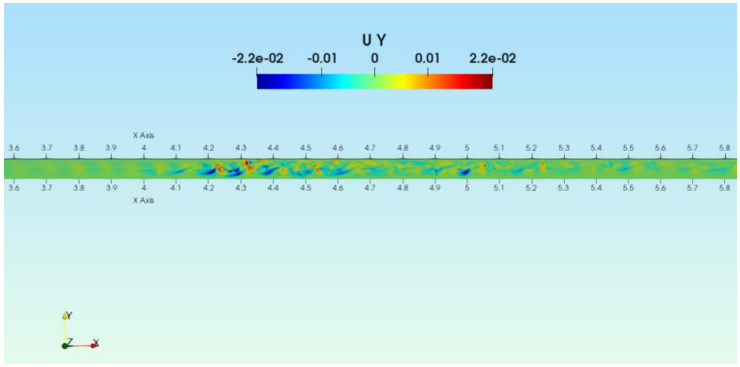

Figure 17. Spanwise velocity at t=470s along the x-axis with respect to the cross-section view cut along the y-axis. Trial 1. Case c (Photo credit: Original)

4.2.4 Analysis of envelopes and peak amplitude

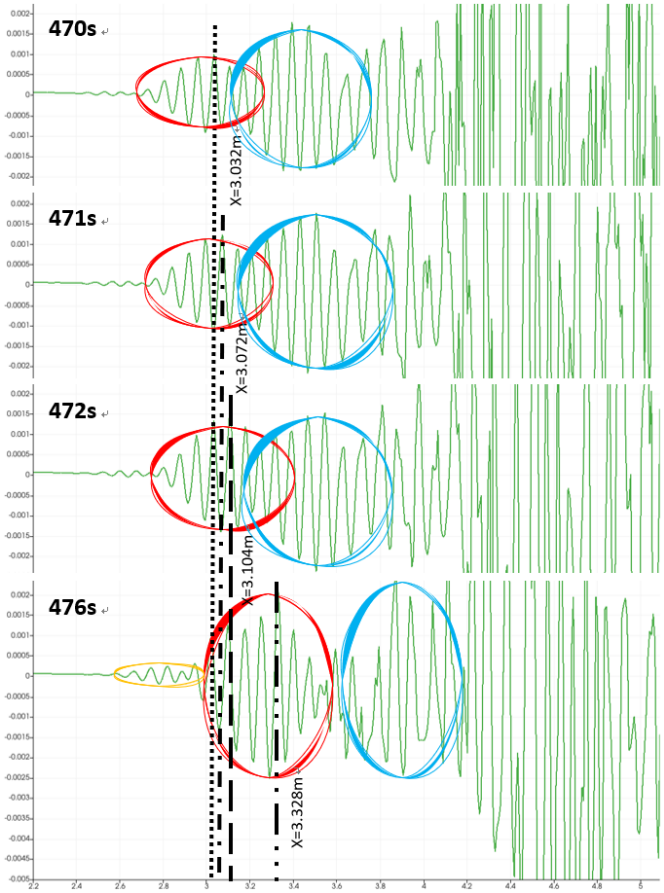

Figure 18. Spanwise velocity, Uy v. s. flow displacement plots at t=470s, 471s, 472s, and 476s, for Trial 1, Case c. The blue, red and yellow circles represent the 1st, 2nd and 3rd envelopes respectively (Photo credit: Original)

As referred to in Fig. 18, several periodic waves will look like bumps at the developing stage called "Envelopes." The wave speed can be quantitively measured and determined by observing the movement of the wave's peak amplitude in a time span. To achieve that, several fixed probes can be utilized to detect that point at different times, or one moving probe can be implemented to increase the accuracy by reducing the influences caused by bulk velocities. Suppose further analysis of the plots of spanwise velocity in the y direction is performed. In that case, it will be found that most of the envelopes form during the developing stage, and new envelopes will continuously form, with old envelopes disappearing from this stage as time goes on. That periodic envelope will eventually fade and become a messy oscillation at the terminal stage. According to Tables 8. and 9., if the movement of peak amplitude can be detected, the wave velocity can be determined, which is about 0.0518m/s higher than the 0.04m/s inlet bulk velocity. In the meantime, the wavelength and frequency of the flow can be obtained, so the differences can be seen if the inlet bulk velocity is varying. For detailed information on the oscillation's wavelength and frequency, please refer to Section 4.2.5.

Table 8. List of peak amplitude's wave speed (for Trial 1, Case c)

Time	**Δl**	**Δt**	**Ux, Peak**
470s-471s	0.04m	1s	0.04m/s
471s-472s	0.032m	1s	0.032m/s
472s-473s	0.04m	1s	0.04m/s
473s-474s	0.032m	1s	0.032m/s
474s-475s	0.112m	1s	0.112m/s
475s-476s	0.04m	1s	0.04m/s
476s-477s	0.032m	1s	0.032m/s
477s-478s	0.04m	1s	0.04m/s
478s-479s	0.12m	1s	0.12m/s
479s-480s	0.03m	1s	0.03m/s
Average UPeak		0.0518m/s	

Table 9. Envelope peak positions at different time points as Ubulk = 0.04m/s

Time Lapse	**2nd Envelope Peak Position @ t=470s**	**2nd Envelope Peak Position @ t=471s**
1 sec	3.032m	3.072m
Time Lapse	**2nd Envelope Peak Position @ t=472s**	**2nd Envelope Peak Position @ t=476s**
4 secs	3.104m	3.328m
Bulk Velocity	0.04m/s	
Wavelength	0.0756 m/period	
Frequency	f = Ubulk/Wavelength = 0.5291Hz	
Period Time	t_{period} = 1/f = 1.89 sec/period	

The wave speed is quantitively determined by observing the movement of the peak amplitude in a range of time. Table 8 lists and Fig. 19 illustrates the change in displacement of the peak amplitude of the travelling flow oscillation each second in a total ten-second span. Hence, the average wave speed is capable of being calculated at about 0.0518m/s. The wave speed of the periodic flow oscillation at the developing stage is faster than the inlet bulk velocity (Ubulk = 0.04m/s). However, the simulated wave speed is no more than 0.04m/s each second, and two time-set data results are offset. The meaning is that the oscillation wave speed is generally lower than the Ubulk, but two abnormal data results (0.112m/s and 0.12m/s) increase the average result. Further research should be focused on double-checking those two abnormal points and deeply analyzing if the causes cause considerable offset data every period. Furthermore, it is also valuable to research whether there are any relationships between those two offset peak amplitude velocities and the flow instability.

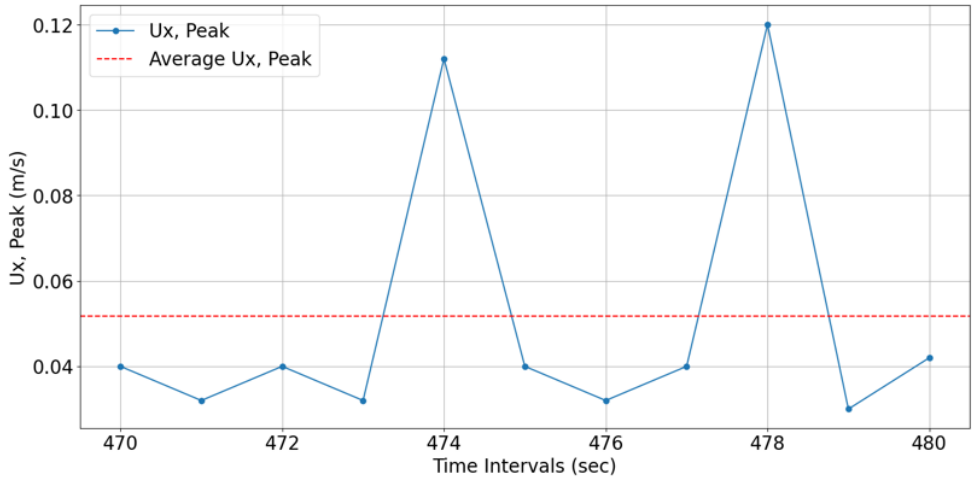

Figure 19. Peak Amplitude Velocity with Time for Trail 1, Case c (Photo credit: Original)

4.2.5 Wavelength and frequency comparison

The characteristics of flow oscillations could be quantitatively investigated by measuring the oscillation wavelengths and frequencies. The wavelength of each case is measured at different seconds via the data displayed on the plots of "Spanwise Velocity, Uy v.s. Flow Displacement" (Fig. 18). For the data results of Trial 1, Case c obtained for wavelength and frequency calculation, please refer to Fig. 18. Wavelength listed in the tables for each case is obtained by averaging the displacement between two adjacent peak amplitudes at different seconds; The wave speed is obtained from Table 9, which is the way to determine the wave speed in this research. The following equation calculates the frequency of flow oscillations [14]:

$$v = \lambda f \tag{5}$$

Table 10. lists the pairs of wavelength and frequency of the Trial 1 Case c scenario every second point in a total ten-second span from t=470s to t=480s. The results obtained from the simulation offer a preliminary reflection that both the wavelength and its frequency are nearly constant at the developing stage in the varying ranges of time if the geometry of the channel and the bulk velocity remain unchanged. As referred to in Table 10., ninety percent of accuracy reflects this specific trial case's wavelength being in a range of (0.075 ± 0.003) m and its frequency being about (0.5357 ± 0.02) Hz, which both seldom vary at different time points; Though all the wavelengths and frequencies are approximately varying with less than 4.2% (errors in wavelengths) and 1.1% (errors in frequencies) differences respectively, the pattern of both wavelength and its frequency at a particular same trial and case are ideally same.

Table 10. List of wavelength and frequency at varying point-in-times for the Trial #1 Case c

Trial #1	Wavelength (m)	Frequency (Hz)
@470s	0.0744	0.53760
@471s	0.0771	0.51890
@472s	0.0752	0.53190
@473s	0.0760	0.52632
@474s	0.0747	0.53570
@475s	0.0747	0.53570
@476s	0.0760	0.52630
@477s	0.0744	0.53763
@478s	0.0742	0.53922
@479s	0.0720	0.55600
@480s	0.0824	0.48540

Table 11. and Fig. 20 demonstrate the pairs of wavelength and frequency at t=470s in four cases (a. Ubulk=0.02m/s, b. Ubulk=0.03m/s, c. Ubulk=0.04m/s, d. Ubulk=0.05m/s). According to Fig. 20,

the wavelength of the flow oscillations is approximately the same, which is about 0.075m at the developing stage, if compared to cases b, c, and d with different bulk velocities at the inlet but the same geometry and its dimensions; Nevertheless, the frequency of the oscillation is observed to be proportional to the Reynolds number. As the bulk velocity in Case b increases to Case c and Case d, the related frequency would be amplified from 0.391Hz to 0.526Hz and 0.682Hz, respectively. It is important to mention that all cases b, c, and d have the existence of flow oscillations observed, excluding Case a, so the first case in the list (Table 11. and Fig. 20) would not be evaluated as a valid data result for the comparison.

Table 11. List of wavelength and frequency at t=470s in four cases

Case #	Peak Uy (m/s)	VRMS (m/s)	Wavelength (m)	Frequency (Hz)
A (0.02m/s)	0.00049591/ -0.0005015	0.00035/ -0.000355	0.089	0.225
B (0.03m/s)	0.00712194/ -0.0112272	0.005036/ -0.00794	0.077	0.391
C (0.04m/s)	0.00748177/ -0.0114015	0.00529/ -0.008062	0.076	0.526
D (0.05m/s)	0.0115081/ -0.0151011	0.00814/ -0.01068	0.073	0.682

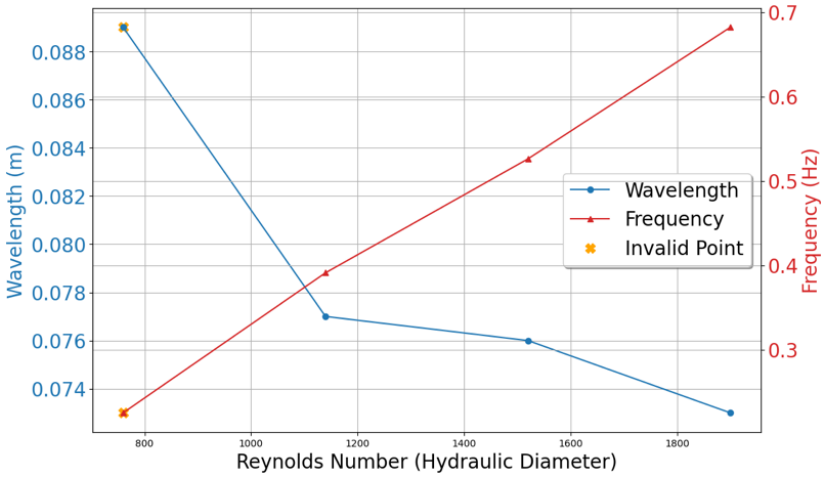

Figure 20. Wavelength and Frequency with Reynolds Number for Cases (Photo credit: Original)

5. Discussion

This simulation model was validated its flow dynamics authenticity by Ethan Sun's previous project [12]. In the meantime, it was testified by simulating the flow in a singular rectangular duct with no slots, and its experimental data results are nearly identical to the theoretical calculations. Furthermore, the verification was also done by doing the grid-dependence test and converging criteria dependence test. Due to the large quantity of grids set for the meshing to increase the accuracy of results, this research requires clusters to assist all the calculations and simulations. Therefore, the clusters held by ComputeCanada would be applied to complete all the simulation calculations by submitting jobs to their terminal station. At the same time, verification and validation were done on the local computer. The current research results gathered reflect the existence of flow pulsations in this singular grooved rectangular channel at the steady state. However, more simulated data results are required to provide a thorough and authentic conclusion, so much work can be done on this topic in the future. For instance, a profile along the x-axis displaying the paths of oscillatory flow oscillated in and out of the continuous groove with vectors is necessary. Moreover, will the change of geometry dimension cause the significant alternation of the locations of the flow oscillation development, or will the relationship of wavelength and frequency be subverted by changing either the geometry

dimension or the bulk velocity? Further certification is required in future works. The step done is to capture visible flow oscillations in the duct and analyze varying bulk velocities causing the oscillation characters, such as frequency and wavelength, to change. The next step scheduled is to thoroughly analyze different cases with different bulk velocities in the same geometry with the same dimension and different dimensions of this geometry with a constant flow rate. It is essential to intensely focus on the development of envelopes in the Uy v.s. Displacement plots, to either see if the number of amplitudes in an envelope will increase or if the wavelength or its moving velocity will vary in one envelope or compared to many envelopes, as time goes in seconds or even in ten seconds.

Further study of this laminar oscillatory flow should focus on wavelength and frequency at several points. The first task is to detect this testing case if the wavelength and its frequency remain nearly unchanged at the developing stage as time goes on. Meanwhile, profoundly observing the process of flow oscillation development is essential to see whether the quantity of the amplitudes in each envelope will increase or not during the flow movement. The second task is to research the influence that would be brought to the wavelength and frequency if the inlet bulk velocity is different. It is crucial to see whether the wavelength and frequency will change hugely if the flow rate is different than that of Case c but with the exact geometry of the channel. The third task is to research the influence that would be brought to wavelength and frequency by adjusting the dimensions of this geometry but keeping the bulk velocity the same as Case c (Ubulk = 0.04m/s). Similar to the second task, the purpose is to detect the possibility of wavelength and frequency changes at different time points if the groove's depth or width changes. For this research study on laminar flow oscillations, a large quantity of data results must be observed from the simulation so a thorough conclusion can be finally made.

The future improvements for this laminar flow oscillation research can be concluded in three points: to test more geometries, implement moving probes, and observe the characteristics of envelopes at the starting and terminal stages rather than at the developing stage. Firstly, additional main channel and groove geometries should be tested so that further data points can be obtained to continuously research the effects of channel width and depth on oscillation behaviors. Secondly, moving probes could be implemented since frequencies measured by fixed probes are affected by bulk velocity. Last but not least, more envelopes at both the starting and terminal stages should be detected and analyzed so their characteristics can be researched entirely with a thorough conclusion or even expectations offered.

6. Nomenclature

U_b = Bulk Velocity
D_h = Hydraulic Diameter
p = Pressure
ρ = Fluid Density
υ = Kinematic Viscosity
μ = Dynamic Viscosity
v = Wave Speed
λ = Wavelength
f = Frequency
U_{Peak} = Velocity of Peak Amplitude
T_{period} = Period Time
Δl = Change in Distance
Δt = Change in Time Lapse
V_{RMS} = Velocity Root Mean Square

7. Conclusion

For this research on modeling and analyzing laminar flow oscillations in a singular grooved channel, we have identified four key achievements based on the data results obtained from the simulations. The initial goal of this study was to confirm the existence and observe the self-sustaining flow oscillations in single grooved channels at a laminar Reynolds number of approximately 750. Oscillatory flows were captured in the 8m-length channel at bulk velocities of 0.03m/s, 0.04m/s, and 0.05m/s, but not at 0.02m/s. The latter requires more time to fully develop before periodic flow pulsations occur. The second finding reveals that the development stages of oscillations shift depending on the inlet bulk velocity; the initial points of each stage are delayed and require a greater distance to form disorganized flow oscillations as the flow rate decreases.

The third finding indicates that while the bulk velocity has minimal impact on the oscillation wavelength, it significantly affects the frequency. The wavelength remains nearly constant across different times despite changes in bulk velocity, yet the frequency consistently increases with the flow rate, showing a proportional relationship. This supports the hypothesis that the rule of frequency being proportional to the Reynolds number in turbulent regimes also holds true in the laminar regime. The fourth discovery is that both the oscillation wavelength and frequency remain nearly constant if the inlet velocity is consistent at different times, suggesting that variations in bulk velocity do not influence the oscillation characteristics, only time does.

However, this study is not without its limitations. One significant drawback is the inability to measure detailed quantitative information without disrupting the flow. Moreover, the study's reliance on simulations means that the experimental validation of these findings is still pending. Real-world applications could introduce factors not accounted for in this simplified model, potentially affecting the reliability of the predictions. Future research should focus on experimental validations and exploring the impact of additional variables, such as channel geometry and surface roughness, to enhance the robustness and applicability of the findings.

References

[1] N. J. Spinks, "Candu Nuclear Power Reactors," A-to-Z Guide to Thermodynamics, Heat and Mass Transfer, and Fluids Engineering, 2011. Available: https://doi.org/10.1615/atoz.c.candu_ nuclear_ power_reactors.

[2] J. D. Hooper, and K. Rehme, "Large-scale structural effects in developed turbulent flow through closely-spaced Rod Arrays," Journal of Fluid Mechanics, vol. 145, no. 1, p. 305, 1984. Available: https://doi.org/10.1017/s0022112084002949.

[3] L. Meyer, and K. Rehme, "Large-scale turbulence phenomena in compound rectangular channels," Experimental Thermal and Fluid Science, vol. 8, no. 4, pp. 286–304, 1994. Available: https://doi. org/10. 1016/0894-1777(94)90059-0.

[4] L. Meyer, and K. Rehme, "Periodic vortices in flow through channels with longitudinal slots or fins," in Tenth Symposium on Turbulent Shear Flows, The Pennsylvania State University, University Park, Pa., USA, Aug. 14-16, 1995.

[5] K. Rehme, "The structure of turbulent flow through Rod Bundles," Nuclear Engineering and Design, vol. 99, pp. 141–154, 1987. Available: https://doi.org/10.1016/0029-5493(87)90116-6.

[6] M. Biemüller, L. Meyer, and K. Rehme, "Large eddy simulation and measurement of the structure of turbulence in two rectangular channels connected by a gap," in Engineering Turbulence Modelling and Experiments, pp. 249–258, 1996. Available: https://doi.org/10.1016/b978-0-444-82463-9.50030-7.

[7] M. Renksizbulut, and G. I. Hadaller, "An experimental study of turbulent flow through a square-array rod bundle," Nuclear Engineering and Design, vol. 91, no. 1, pp. 41–55, 1986. Available: https: //doi.org/10.1016/0029-5493(86)90183-4.

[8] Y. Fen Shen, Z. Dong Cao, and Q. Gang Lu, "An investigation of crossflow mixing effect caused by grid spacer with mixing blades in a rod bundle," Nuclear Engineering and Design, vol. 125, no. 2, pp. 111–119, 1991. Available: https://doi.org/10.1016/0029-5493(91)90071-o.

[9] S. H. Hong, J. S. Seo, J. K. Shin, and Y. D. Choi, "Numerical investigation of turbulent flow pulsation in compound rectangular channels," in Proceeding of Sixth International Symposium on Turbulence and Shear Flow Phenomena, 2009. Available: https://doi.org/10.1615/tsfp6.810.

[10] J. Goulart, L. Noleto, and S. V. Möller, "Experimental study of mixing layer in a closed compound channel," Journal of the Brazilian Society of Mechanical Sciences and Engineering, vol. 36, no. 2, pp. 411–420, 2013. Available: https://doi.org/10.1007/s40430-013-0081-3.

[11] A. Gosset, and S. Tavoularis, "Laminar flow instability in a rectangular channel with a cylindrical core," Physics of Fluids, vol. 18, no. 4, 2006. Available: https://doi.org/10.1063/1.2194968.

[12] S. Ethan, "Modeling Laminar Oscillatory Flow in Single Grooved Channels," unpublished, 2021.

[13] M. S. Guellouz, F. Souissi, and N. Ben Salah, "The flow structure in the narrow gaps of compound channels: The basic flow," Arabian Journal for Science and Engineering, vol. 45, no. 7, pp. 5447–5458, 2020. Available: https://doi.org/10.1007/s13369-020-04433-6.

[14] Halliday, D., Resnick, R., & Walker, J. (2001). Fundamentals of physics. Wiley.